Summarizing the results, we draw the following conclusions. In the experimental investigation of heat-transfer processes on the basis of a limited volume of initial data it is possible to determine simultaneously a set of parameters that do not violate the one-to-one correspondence with given observations. The experimental assurance of the conditions necessary for this objective permits the specific heat and thermal conductivity to be determined simultaneously without using volume heat sources, or likewise the thermophysical properties and transient boundary heat fluxes, and additionally the heat-transfer coefficient to be reconstructed. What this means in practice is the possibility of enlarging the volume of information obtainable in the interpretation of experimental results by conventional methods. It must also be borne in mind that among the solutions of the heat-conduction equation there exists a subset that imparts ambiguity to the determination of the coefficients of the mathematical model. The existence of that subset is attributable to the invariant properties of the solution of the boundary-value problem with respect to its coefficients. The resulting necessary conditions for the existence of an unidentifiable temperature field can be applied directly in practice.

NOTATION

x, space coordinate; t, time; Q_T, domain of independent variables; T, upper time limit; a_1, specific heat; a_2, thermal conductivity; a_3, heat-transfer coefficient; f, power of volume heat sources; φ, initial temperature distribution; $v_{0,1}$, boundary functions; q, q_0, q_1, heat flux; u, temperature field; u^*, unidentifiable state; $\lambda_{1,2}$, ρ, ρ_1, ρ_2, parameters of family from ambiguity subset; C^1, C^2, $C^{2,1}$, classes of differentiable functions.

LITERATURE CITED

1. V. A. Osipova, Experimental Investigation of Heat-Transfer Processes [in Russian], Énergiya, Moscow (1969).
2. A. G. Shashkov, G. M. Volokhov, T. N. Abramenko, and V. P. Kozlov, Methods for Determining the Thermal Conductivity and Thermal Diffusivity [in Russian], Énergiya, Moscow (1973).
3. M. R. Romanovskii, "Identifiability of mathematical models," Izv. Akad. Nauk SSSR, Tekh. Kibern., No. 6, 192-193 (1980).
4. M. R. Romanovskii, "Uniqueness of the solution of the inverse coefficient problem for a linear heat-conduction equation," Inzh.-Fiz. Zh., 42, No. 3, 476-483 (1982).

MATHEMATICAL SIMULATION OF THERMOGRAVITATIONAL CONVECTION IN SOLIDIFICATION OF LIQUID STEEL

Yu. A. Samoilovich, L. N. Yasnitskii, and Z. K. Kabakov

UDC 536.25:621.746

The thermal and hydrodynamic phenomena accompanying crystallization of liquid steel are analyzed numerically.

It is well known that the major portion of defects in castings develop during the phase transition of the alloy from the liquid to the solid state. Direct experimental study of the thermal and especially the hydrodynamic phenomena accompanying the steel crystallization process is difficult because of the thermal and chemical aggressiveness of liquid steel. Thus, the role of mathematical simulation becomes important in study of this process.

Metallic alloys are inclined to produce dendrite forms of crystal growth, leading to formation of a two-phase zone which is a mixture of liquid alloy and branches of the growing dendrites. Thus, within the solidifying alloy one can always distinguish three regions with different aggregate metal states — a zone of completely solidified metal, a zone of liquid alloy, and a two-phase zone separating the former ones (Fig. 1).

All-Union Scientific-Research Institute of Metallurgical Thermotechnology, Sverdlovsk. Perm State Unversity.

Translated from Inzhenerno-Fizicheskii Zhurnal, Vol. 44, No. 3, pp. 465-473, March, 1983. Original article submitted January 11, 1982.

0022-0841/83/4403-0326$07.50

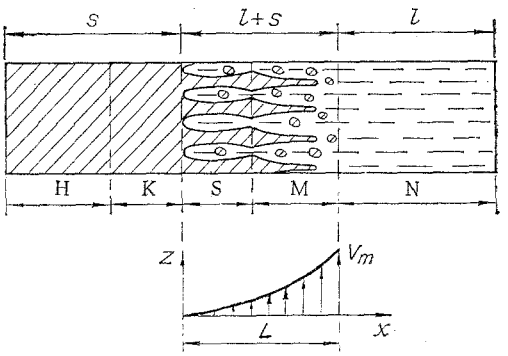

Fig. 1. Diagram of alloy solidification: s) solid alloy region; l) liquid region; l + s) two-phase zone. H, K, S, M, N) regions of alloy described by Hooke, Kelvin, Shvedov, Maxwell, and Newton rheological models. Below, alloy motion through two-phase zone.

Motion of the unsolidified metal takes place in both the liquid and the two-phase regions of the casting, although the flow regime in those two regions differ significantly. While in the liquid region the melted metal is free of crystallized particles and its behavior, judging from numerous ezperimental results [1-4], can be described satisfactorily by the equations of motion of a Newtonian liquid, in the two-phase zone free motion of the liquid is hindered by a network of growing dendrites, and the physical properties of the melted metal change because of the large number of suspended solid particles. In addition, we must consider that the flow in the two-phase region takes place under complex conditions of shrinkage in the crystallizing metal and formation of shrinkage pores. This all places the solidifying alloy in the two-phase zone in a partially stressed state and causes the alloy to manifest elasticity and compressibility properties which are not described by the Navier–Stokes law. Naturally, the concept of a Newtonian liquid loses force under these conditions, and the equations of motion of the alloy must consider its rheological properties.

The solidifying metal has been represented by a number of rheological models [2, 5-7]. The completely solidified portion of the casting, cooled to temperatures below 800-900°K, can to a great degree of accuracy be considered and absolutely elastic body, which follows the classical Hooke's law. In the unsolidified portion, in the presence of only slight superheating, the behavior of the liquid metal is described satisfactorily by Newton's viscous friction law. Between these two limits the behavior of the solidifying metal passes through an entire spectrum of states from a Newtonian body to a Hooke body, as shown schematically in Fig. 1.

Depending on the particular problem under investigation, researchers accent one or the other rheological model of the metal. For example, study of the stressed state of the solid shell of a casting in connection with the development of clod cracks is performed using the theory of elasticity. In analysis of hot crack formation [5], a model proposed by Kashirtsev [6] has been used, which in dependence on the intensity of loading can degenerate into an elastic Hooke body, a viscoelastic Maxwell liquid, or a plastic Shvedov body. Finally, to describe convective phenomena in the liquid core of a casting the differential equations of the hydrodynamics of a viscous incompressible Newtonian liquid have been used [8-15].

Choosing the goal of analyzing the conditions of interaction between the two-phase zone and the convective flow of the alloy within the liquid core of the casting, we take as a working hypothesis that the behavior of the two-phase zone can be described by Maxwell's viscoelastic liquid model. It is obvious that this hypothesis is sufficiently accurate for that portion of the two-phase zone adjoining the two-phase zone – liquid metal boundary, where the solidifying alloy is in intense motion and the properties of viscoelasticity are dominant.

The differential equation for the motion of a Maxwell liquid can be derived by using the equations of the dynamics of continuous media [16, p. 62].

$$\rho \frac{D\mathbf{V}}{D\tau} = \rho \mathbf{F} + \mathrm{Div}\, P. \tag{1}$$

We differentiate Eq. (1) with respect to time and multiply both sides by the constant τ_R, which defines the relaxation time of the medium:

$$\tau_R \frac{D\rho}{D\tau}\frac{D\mathbf{V}}{D\tau} + \tau_R \rho \frac{D^2\mathbf{V}}{D\tau^2} = \tau_R \mathbf{F}\frac{D\rho}{D\tau} + \tau_R \frac{D\mathbf{F}}{D\tau} + \mathrm{Div}\left(\tau_R \frac{DP}{D\tau}\right). \tag{2}$$

Combining Eqs. (1) and (2), we obtain

$$\rho\left(\frac{D\mathbf{V}}{D\tau} + \tau_R \frac{D^2\mathbf{V}}{D\tau^2}\right) + \tau_R \frac{D\rho}{D\tau}\frac{D\mathbf{V}}{D\tau} = \rho\left(\mathbf{F} + \tau_R \frac{D\mathbf{F}}{D\tau}\right) + \tau_R \mathbf{F}\frac{D\rho}{D\tau} + \mathrm{Div}\left(P + \tau_R \frac{DP}{D\tau}\right). \tag{3}$$

We define the relationship between the stress tensor P and the deformation rate tensor $\dot{S}$ by a generalized rheological Maxwell law, written for an isotropic compressible medium:

$$P + \tau_R \frac{DP}{D\tau} = 2\mu\dot{S} - \left(p + \tau_R \frac{Dp}{D\tau} + \frac{2}{3}\mu \operatorname{div}\mathbf{V}\right)E. \tag{4}$$

After substitution of Eq. (4) in Eq. (3), we obtain

$$\rho\left(\frac{D\mathbf{V}}{D\tau} + \tau_R \frac{D^2\mathbf{V}}{D\tau^2}\right) + \tau_R \frac{D\rho}{D\tau} = \rho\left(\mathbf{F} + \tau_R \frac{D\mathbf{F}}{D\tau}\right) + \tau_R \mathbf{F}\frac{D\rho}{D\tau} -$$
$$-\nabla\left(p + \tau_R \frac{Dp}{D\tau}\right) + (\nabla\mu\nabla)\mathbf{V} - \frac{2}{3}\nabla\mu(\nabla\mathbf{V}) + \left(\nabla\mu\frac{d\mathbf{V}}{d\mathbf{r}}\right). \tag{5}$$

Equation (5) is the hydrodynamic equation of a viscoelastic compressible liquid. In the special case in which $\tau_R = 0$, div $\mathbf{V}=0$, and μ = const, Eq. (5) transforms to the equation of motion of a viscous incompressible Newtonian liquid [16, p. 362]. The most significant difference between the equation obtained here and the equation of motion of a Newtonian liquid is the presence of the second derivative of velocity with respect to time, which gives the equation of hyperbolic form. This imposes corresponding unique features upon the character of the nonstationary solutions obtainable.

We will analyze Eq. (5) for the one-dimensional case of liquid metal motion within the limits of a two-phase zone of thickness L, as depicted in Fig. 1. Neglecting the derivatives of the flow velocity along all coordinates except x, and also changes in pressure and density, we obtain the equation for transfer of quantity of motion in the form

$$\rho\left(\frac{\partial V_z}{\partial\tau} + \tau_R \frac{\partial^2 V_z}{\partial\tau^2}\right) = \frac{\partial}{\partial x}\left(\mu\frac{\partial V_z}{\partial x}\right). \tag{6}$$

In solving nonstationary differential equation (6), one must specifiy certain initial velocity and acceleration values, for example:

$$V_z = 0, \quad \frac{\partial V_z}{\partial\tau} = 0 \quad \text{at} \quad \tau = 0. \tag{7}$$

On the boundaries of the two-phase zone boundary conditions for the velocity are specified:

$$V_z = 0 \quad \text{at} \quad x = 0 \text{ and } V_z = V_m \quad \text{at} \quad x = L. \tag{8}$$

We take the change in the viscosity coefficient μ over the thickness of the two-phase zone in the form of a power series in the parameter Ψ:

$$\mu = \mu_0 \sum_{n=0}^{\infty} A_n \Psi^n. \tag{9}$$

When the first two terms of series (9) are used, we obtain the well-known Einstein expression, valid for weakly concentrated suspensions:

$$\mu = \mu_0(1 + 2{,}5\Psi). \tag{10}$$

However, as was noted by Leonova [7], Eq. (10) does not agree with experimental data on the properties of solidifying melts. Data are presented in [5] on the distribution of effective viscosity in the two-phase zone of an alloy Al + 0.6% Si, which can be approximated with sufficient accuracy by the polynomial

$$\mu = \mu_0(1 + 2{,}5\Psi + A\Psi^4). \tag{11}$$

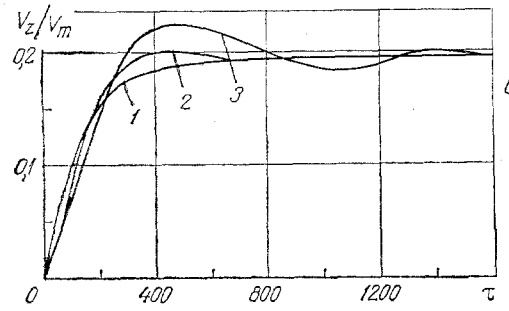

Fig. 2

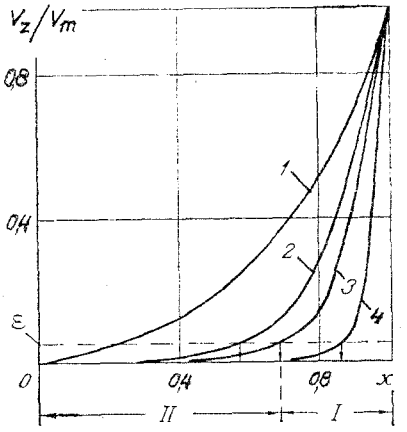

Fig. 3

Fig. 2. Flow velocity vs time at two-phase zone point x = 0.075 m for various relaxation times: 1) $\tau_R = 0$; 2) 50; 3) 100. A = 250.

Fig. 3. Stationary distribution of velocity in two-phase zone for various A in viscosity distribution law (11): 1) A = 0; 2) 250; 3) 1000; 4) 10,000.

The coefficient A in Eq. (11) characterizes the increase in viscosity upon transition of the alloy from the liquid to the solid state.

It follows from analysis of experimental data [6, 7, 17] that the effective viscosity coefficient depends to a great degree on the chemical composition of the alloy, as reflected in a change in A from 240 to 10,000.

Numerical integration of differential equation (6) with specified boundary conditions (7), (8) and viscosity distribution law (11) was carried out by the finite difference method using the Dufort—Frankel technique [18]. Calculations were performed for the following initial parameter values: $\mu_0 = 4.2 \cdot 10^{-3}$ N·sec/m^2; $\rho = 7 \cdot 10^3$ kg/m^3; L = 0.1 m.

Figure 2 depicts the process of establishment of a stationary flow regime with variation of the relaxation time (τ_R). The control parameter chosen was the flow velocity (V_z) at a point within the two-phase medium located a distance of 1/4L from the liquidus boundary. As follows from the figure, with increase in the parameter τ_R the time required for establishment of a stationary flow regime in the Maxwell liquid increases.

Figure 3 shows the stationary velocity distribution in the two-phase zone for various values of the coefficient A in the viscosity distribution law (11). As is evident from the figure, the flow velocity of the solidifying metal in the two-phase zone falls off abruptly near the liquidus boundary and then tends smoothly toward zero with approach to the boundary x = 0.

The results obtained on liquid metal behavior in the two-phase zone can be used to formulate boundary conditions for study of hydrodynamic phenomena in the liquid core of the solidifying casting. To do this we introduce the concept of an arbitrary solidification boundary, commencing from the concept that beyond the limits of this boundary the displacement rate of the melt comprises a relatively small fraction ε of the maximum perturbed flow velocity V_m, i.e., $V_z \leqslant V_*$, where $V_* = \varepsilon V_m$. Choosing, for example, ε = 0.05, we find from Fig. 3 that the solidification boundary is determined by the coordinate $X_* = 0.7 - 0.8$. In the region $X_* < X < 1$ the melt displacement rate exceeds the critical value V_*.

It should be noted that the solidification boundary defined here is equivalent to the concept of a pourability boundary introduced by Gulyaev [19]. The experimental data of [19], obtained by turning over partially solidified castings of an iron alloy, indicate that the pourability boundary occurred at the value Ψ = 0.3, so that X = 1 — Ψ = 0.7, which coincides with the solidification boundary obtained in our calculations.

The analysis performed justifies division of the two-phase zone of the casting into two regions separated by a pourability (solidification) region. Within the limits of region 1

(Fig. 3) within the limits of region I (see Fig. 3) the liquid flow velocity decreases monotonically from V_m to $V_* \approx 0$, while in region II motion of the melt can be neglected in practice. Thus we have a two-element description of the two-phase zone, which permits use of the differential equations of a Newtonian liquid for description of the motion of the unsolidified metal over the entire region in the casting where the temperature is above the pourability temperature ($T > T_E$). On the pourability boundary we must require the adhesion condition

$$\mathbf{V} = 0 \quad \text{at} \quad T = T_E . \tag{12}$$

After these preliminary remarks, we now turn to formulation of the combined problem of the hydrodynamics and heat exchange of the solidifying metal, which requires simultaneous solution of the following differential equations.

1. The heat-transfer equations for the liquid, solid, and solid–liquid states of the alloy, written with consideration of heat liberation due to phase transition in the liquid–solidus temperature interval ($T_l - T_s$)

$$\frac{\partial T}{\partial \tau} + V_x \frac{\partial T}{\partial x} + V_z \frac{\partial T}{\partial z} = \frac{\lambda}{\rho c_{ef}} \left(\frac{\partial^2 T}{\partial x^2} + \frac{\partial^2 T}{\partial z^2} \right). \tag{13}$$

Here c_{ef} is the effective specific heat which is specified as a function of alloy temperature in accordance with the technique of calculating heat of crystallization in the two-phase zone [15].

2. The system of Navier–Stokes hydrodynamics equations, written in the Boussinesq approximation:

$$\frac{\partial V_x}{\partial \tau} + V_x \frac{\partial V_x}{\partial x} + V_z \frac{\partial V_x}{\partial z} = -\frac{1}{\rho} \frac{\partial p}{\partial x} + \nu \left(\frac{\partial^2 V_x}{\partial x^2} + \frac{\partial^2 V_x}{\partial z^2} \right), \tag{14}$$

$$\frac{\partial V_z}{\partial \tau} + V_x \frac{\partial V_z}{\partial x} + V_z \frac{\partial V_z}{\partial z} = -\frac{1}{\rho} \frac{\partial p}{\partial z} + \nu \left(\frac{\partial^2 V_z}{\partial x^2} + \frac{\partial^2 V_z}{\partial z^2} \right) + g\beta (T - T_E), \tag{15}$$

$$\frac{\partial V_x}{\partial x} + \frac{\partial V_z}{\partial z} = 0 \quad \text{(continuity equation).} \tag{16}$$

The algorithm used to solve the equations is constructed so that Eqs. (14)-(16) are solved simultaneously with thermal conductivity equation (13) in that portion of the casting in which up to the given time the temperature has not yet fallen to the pourability temperature ($T > T_E$). In the portion of the casting in which crystallization has begun, where the temperature is below the pourability temperature ($T \leqslant T_E$) only the thermal conductivity equation (13) is solved; the velocity field is assumed equal to zero. Thus, on the crystallization front fixed by the pourability isotherm ($T = T_E$), the position of which is determined at any time by a combination of thermal and hydrodynamic circumstances, adhesion condition (12) is satisfied.

In the numerical realization of these differential equations, an approach was employed which is sometimes termed the artificial compressibility method [20]. In accordance with this technique, in the computation algorithm continuity equation (16) is formally replaced by the equation

$$\frac{\partial p}{\partial \tau} + n_p \left(\frac{\partial V_x}{\partial x} + \frac{\partial V_z}{\partial z} \right) = 0, \tag{17}$$

in which the parameter n_p is chosen during the calculation process. This approach presumes organization of an additional iteration process at each time layer, as a result of which a pressure field and corresponding velocity field are defined, which approximately satisfy continuity equation (16).

Numerical integration of differential equations (13)-(17) was accomplished by the finite-element method [21, 15], in which the calculation region is covered by a grid consisting of triangular elements, and the desired functions are repesented by linear functions of the coordinates within each element. The algorithm for numerical integration of these equations by the finite element method using the artifical compressibility technique, smoothing over space and averaging in time, was described in detail in [15, 21, 22].

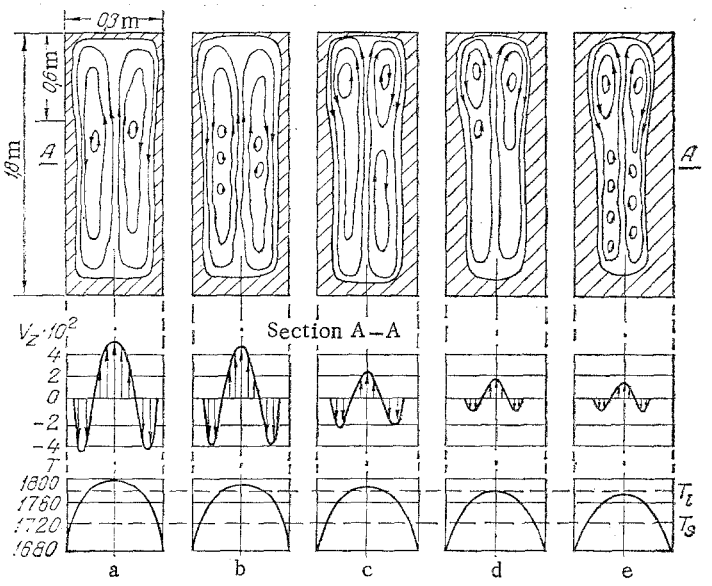

Fig. 4. Flow function isoline patterns (above) and longitudinal velocity V_z and temperature T profiles for times: a) τ = 600 sec; b) 900; c) 1800; d) 3600; e) 5400. Solidified metal region is cross-hatched. V_z, m/sec, T, °K.

In the calculations presented below, the following physical characteristics were used for carbon steel: T_l = 1781°K, T_s = 1723°K, T_E = 1763°K, c_l = 800 J/(kg·deg K), c_s = 660 J/(kg·deg K), $\mathcal{L}$ = 272,000 J/kg, λ = 29 W/(m·deg K), $\beta = 0.17 \cdot 10^{-3}$ deg K^{-1}, $\nu = 0.6\ 10^{-6}$ m^2/sec.

The mathematical model described was used to study the process of solidification of a casting of most simple form — a plate with distance between the wide edges 2S = 0.3 m and height H = 1.8 m, cast in a sand–clay form. The upper head portion of the casting with h = 0.6 m was surrounded by a thermal insulation mixture.

It is known from experiment that in the initial period of cast crystallization the surface temperature falls abruptly, and then remains constant during practically the entire solidification process. Therefore, as boundary conditions on that portion of the casting surface in contact with the sand–clay form, we choose a constant temperature T_1 = 1673°K, while on the portion in contact with the thermal insultation, T_2 = 1723°K.

At the initial moment the alloy in the calculated region is assumed at rest with an initial temperature, constant over volume, of T_0 = 1803°K:

$$V_x = 0, \quad V_z = 0, \quad T = T_E \quad \text{at} \quad \tau = 0. \tag{18}$$

The results of calculating the thermal and hydrodynamic quantities are presented in Fig. 4 in the form of flow function isolines and vertical velocity component profiles in a middle cross section of the casting at various times. As is evident from the figure, the liquid metal sinks at the side walls of the casting and rises in the central portion with formation of two circulation contours. Such a pattern of thermogravitational convection in solidification of steel was described in [8-14]. Less well known is the fact of formation within the circulation contours of a series of fine vortices which appear and disappear during the process of reduction in size of the liquid casting core. Of interest is the order which appears in the vortex positions, which we may arbitrarily term "chessboard" order.

Liquid flow with chessboard vortex configuration is a phenomenon observed frequently in nature (for example, the Karman vortex path). In [23] observations of turbulent liquid motion on the boundary between meeting flows was described: the vortex formations arrange themselves in chessboard order, despite the symmetrical conditions under which the experiment was performed. The development of asymmetrical chessboard motion of the liquid in the present case can be explained by the fact that the symmetrical flow pattern existing in the initial stage of the process loses its stability under the action of random perturbing factors (vibrations, channel wall roughness), and transforms to an energetically more favorable asymmetric pattern.

A similar situation occurs in the mathematical simulation: with absolutely symmetric boundary conditions, computer solution of the problem shows rearrangement of the flow lines into the asymmetrical chessboard pattern. Such a pattern was observed, for example, by Yakimov [24], who utilized rounding errors at the points of the finite-difference grid as the perturbing factor. The appearance of chessboard structure in vortex locations in a vertical channel was established analytically by Gershun and Zhukhovitskii [25].

In the present study our mathematical simulation has found formation of a chessboard structure in the liquid steel convection during solidification of the casting. The fact that this phenomenon has not been observed in similar theoretical studies [9-15] can be explained by the fact that hydrodynamic field symmetry was always imposed about the casting axis, eliminating asymmetrical liquid convection forms.

It should be noted that the phenomenon of vortex formation in the liquid core of a casting has a direct relationship to the process of segregation of impurities and formation of chemical inhomogeneities in the cast metal. In particular, the vortices stimulates additional mixing of the liquid, intensifying heat and mass transfer in the horizontal direction. Moreover, impurities and nonmetallic inclusions are attracted into the rarefied zone formed by the rotating metal and accumulate in the central portion of the vortices.

In analyzing Fig. 4 one notes that despite the complex character of the convection, the profile of the vertical component of the velocity vector in the central cross section has a simple symmetrical form, which can be approximated by the following expression with satisfactory accuracy:

$$V_z = V_0\left[1 - 2(n+1)\left(\frac{x}{b}\right)^n + (2n+1)\left(\frac{x}{b}\right)^{2n}\right], \quad 0 \leqslant x \leqslant b, \; n = 2. \tag{19}$$

Equation (19) can be used to develop simplified methods for calculating metal solidification.

Thus, by solving the combined problem of heat exchange and hydrodynamics, new information has been obtained on the character of metal motion in the liquid core of a solidying casting. The phenomenon of formation of a series of vortices within the overall circulation contours has been established. The vortices are arrayed in a "chessboard" order. An equation has been proposed for description of the longitudinal velocity profile in the central section of the casting.

NOTATION

x, y, planar Cartesian coordinates; τ, time; T, alloy temperature; V_x, V_y, horizontal and vertical components of velocity V; ρ, λ, c_{ef}, ν, μ, β, density, thermal conductivity, effective specific heat, kinematic and dynamic viscosities, thermal expansion coefficients; $g = 9.8$ m/sec^2, acceleration of gravity; p, pressure; T_ℓ, T_S, T_E, liquid, solidus, and pourability temperatures; c_ℓ, c_S, specific heats of liquid and solid alloy phases; L, specific heat of crystallization; 2S, H, casting thickness and height; h, mold head height; V_0, ascending flow velocity on casting axis (at x = 0); b, thickness of casting liquid core; F, volumetric force distribution density; P, S, stress and deformation rate tensors; τ_R, Maxwell liquid relaxation time; E, tensor unit; Ψ, relative quantity of solid phase in elementary melt volume; θ, dimensionless temperature; X, dimensionless coordinates; L, thickness of two-phase zone; n_r, relaxation parameter.

LITERATURE CITED

1. E. Z. Rabinovich, "Experimental study of motion of fused metal in an open channel," Dokl. Akad. Nauk SSSR, 54, No. 3, 201-203 (1946).
2. B. V. Rabinovich, Introduction to Casting Hydraulics [in Russian], Mashinostroenie, Moscow (1966).
3. V. M. Borishanskii and S. S. Kutateladze, "Calculation of heat transfer and hydraulic resistance in flow of liquid metals in tubes," Energomashinostroenie, No. 6, 58-62 (1957).
4. V. M. Borishanskii and S. S. Kutateladze, "Heat transfer and hydraulic resistance in flow of liquid metals," Zh. Tekh. Fiz., 28, No. 4, 836-847 (1958).
5. G. F. Balandin, Fundamentals of Casting Formation Theory [in Russian], Mashinostroenie, Moscow (1979).

6. G. F. Balandin and L. P. Kashirtsev, "Study of structural-mechanical properties of aluminum–silicon alloys in the crystallization interval," in: Casting Properties of Alloys [in Russian], Naukova Dumka, Kiev (1968), pp. 228-240.
7. E. A. Leonova, "Mechanical properties of metals in the vicinity of the crystallization temperature," in: Elasticity and Inelasticity [in Russian], Vol. 1, Moscow State Univ. (1971), pp. 221-252.
8. G. A. Ostroumov, Free Convection Under Internal Problem Conditions [in Russian], Gostekhteorizdat, Moscow–Leningrad (1952).
9. I. L. Povkh, É. A. Iodko, and P. F. Zavgorodnii, "Study of thermal gravitational convection and its effect on heat-mass transfer processes in solidifying melts," Tepolofiz. Vys. Temp., 16, No. 6, 1250-1257 (1978).
10. Yu. A. Samoilovich, "Hydrodynamic phenomena in the unsolidified portion (liquid core) of a casting," Izv. Akad. Nauk, SSSR, Met., No. 2, 84-92 (1969).
11. B. I. Vaisman and E. L. Tarunin, "Effect of crystallization on the free convection process in fused metals," Uch. Zap. Perm. Univ., No. 293, 107-118 (1972).
12. P. G. Kroeger and S. Ostrach, "The solution of a two-dimensional freezing problem including convection effects in liquid region," Int. J. Heat Mass Transfer, 17, No. 10, 1191-1207 (1974).
13. S. Asai and J. Szekely, "Turbulent flow and its effects in continuous casting," Ironmaking Steelmaking, 2, No. 3, 205-213 (1975).
14. B. I. Myznikova and E. L. Tarunin, "Free convection in fused metals during crystallization," in: Mathematical Methods in the Study of Special Electrometallurgy Processes [in Russian], Naukova Dumka, Kiev (1976), pp. 129-136.
15. Yu. A. Samoilovich, L. N. Yasnitskii, and Z. K. Kabakov, "Composite problem of heat exchange and hydrodynamics in a solidifying melt," Teplofiz. Vys. Temp., 19, No. 4, 814-820 (1981).
16. L. G. Loitsyanskii, Liquid and Gas Mechanics [in Russian], Nauka, Moscow (1978).
17. E. G. Shvidovskii, Some Questions on the Viscosity of Fused Metals [in Russian], Gostekhizdat (1955).
18. R. D. Richtmyer and K. W. Morton, Difference Methods for Initial-Value Problems, Wiley (1967).
19. B. B. Gulyaev, Theory of Casting Processes [in Russian], Mashinostroenie, Leningrad (1976).
20. A. J. Chorin, "Numerical solution of the Navier–Stokes equation," Math. Comp., 22, No. 104, 745-762 (1968).
21. Yu. A. Samoilovich and L. N. Yasnitskii, "Algorithm for solution of problems of thermogravitational convection of a viscous incompressible liquid by the finite element method," Dep. VINITI No. 1131-80.
22. Yu. A. Samoilovich and L. N. Yashnitskii, "Method for stabilization of the numerical solution of nonstationary Navier–Stokes equations in the high Reynolds number range," dep. VINITI, No. 19194-81.
23. V. G. Kozlov, "Stability of periodic liquid motion in a plane channel," Izv. Akad. Nauk SSSR, Mekh. Zhidk, Gaza, No. 6, 114-118 (1979).
24. A. A. Yakimov, "Secondary convection flows in a plane vertical liquid layer with internal heat sources," in: Hydrodynamics. Proceedings of Perm Pedagogical Institute [in Russian], Vol. 7, Perm. Knizh. Izd., Perm (1974), pp. 53-63.
25. G. Z. Gershuni and E. M. Zhukovitskii, Convective Stability of Incompressable Fluids, Halsted Press (1976).